

REPORT DOCUMENTATION PAGE				Form Approved OMB No. 0704-0188	
<p>The public reporting burden for this collection of information is estimated to average 1 hour per response, including the time for reviewing instructions, searching existing data sources, gathering and maintaining the data needed, and completing and reviewing the collection of information. Send comments regarding this burden estimate or any other aspect of this collection of information, including suggestions for reducing the burden, to the Department of Defense, Executive Services and Communications Directorate (0704-0188). Respondents should be aware that notwithstanding any other provision of law, no person shall be subject to any penalty for failing to comply with a collection of information if it does not display a currently valid OMB control number.</p> <p><b>PLEASE DO NOT RETURN YOUR FORM TO THE ABOVE ORGANIZATION.</b></p>					
1. REPORT DATE (DD-MM-YYYY) 19 Mar 2008		2. REPORT TYPE FINAL REPORT		3. DATES COVERED (From - To) 01 Jun 2006 - 30 Nov 2007	
4. TITLE AND SUBTITLE (NANOTECHNOLOGY INIATIVTE) MULTICOLOR NANOSTRUCTURED HIGH EFFICIENCY PHOTOVOLTAIC DEVICES				5a. CONTRACT NUMBER FA9550-06-1-0447	
				5b. GRANT NUMBER 06NE112	
				5c. PROGRAM ELEMENT NUMBER	
6. AUTHOR(S) Dr. Christiana Honsberg				5d. PROJECT NUMBER	
				5e. TASK NUMBER	
				5f. WORK UNIT NUMBER	
7. PERFORMING ORGANIZATION NAME(S) AND ADDRESS(ES) UNIVERSITY OF DELAWARE				8. PERFORMING ORGANIZATION REPORT NUMBER	
9. SPONSORING/MONITORING AGENCY NAME(S) AND ADDRESS(ES) AF OFFICE OF SCIENTIFIC RESEARCH 875 NORTH RANDOLPH STREET ROOM 3112 ARLINGTON VA 22203 <i>Dr Kitt Reinhardt/NE</i>				10. SPONSOR/MONITOR'S ACRONYM(S)	
				11. SPONSOR/MONITOR'S REPORT NUMBER(S)	
12. DISTRIBUTION/AVAILABILITY STATEMENT DISTRIBUTION STATEMENT A: UNLIMITED				AFRL-SR-AR-TR-08-0228	
13. SUPPLEMENTARY NOTES					
14. ABSTRACT <p>The goal of the project "Multicolor Nanostructured High Efficiency Photovoltaic Devices," is to experimentally demonstrate the fundamental physical mechanisms required for high performance photovoltaics, focusing on the conditions which maximize simultaneous radiative coupling between multiple energy levels. A material which has multiple quasi-Fermi levels is predicted to display a range of unique properties, including highly nonlinear absorption coefficients which depend on light intensity, absorption and emission properties which can be tuned by shining different wavelengths of light on the material, and the ability to alter the mobility of one type of carrier while leaving the other unaffected. While these properties allow a range on new devices, the focus of the material choices and theory is on ultra-high efficiency photovoltaics. Other potential new devices include efficient broad-band emitters, and lasers and photodetectors which are multicolor and switchable between the operating wavelengths.</p>					
15. SUBJECT TERMS Photovoltaic Devices					
16. SECURITY CLASSIFICATION OF:			17. LIMITATION OF ABSTRACT	18. NUMBER OF PAGES 14	19a. NAME OF RESPONSIBLE PERSON
a. REPORT	b. ABSTRACT	c. THIS PAGE			19b. TELEPHONE NUMBER (Include area code)

## **Multicolor Nanostructured High Efficiency Photovoltaic Devices**

**AFSOR Subcontract #FA9550-06-1-0047**

**Annual Performance Report 30 June 2007**

**C. Honsberg, S.P. Bremner, G.M. Liu, K.Y. Ban**

### **Summary**

The goal of the project “*Multicolor Nanostructured High Efficiency Photovoltaic Devices*,” is to experimentally demonstrate the fundamental physical mechanisms required for high performance photovoltaics, focusing on the conditions which maximize simultaneous radiative coupling between multiple energy levels. A material which has multiple quasi-Fermi levels is predicted to display a range of unique properties, including highly non-linear absorption coefficients which depend on light intensity, absorption and emission properties which can be tuned by shining different wavelengths of light on the material, and the ability to alter the mobility of one type of carrier while leaving the other unaffected. While these properties allow a range on new devices, the focus of the material choices and theory is on ultra-high efficiency photovoltaics. Other potential new devices include efficient broad-band emitters, and lasers and photodetectors which are multicolor and switchable between the operating wavelengths

Despite the theoretical promise of multiple-quasi-Fermi level materials, the basic physical effect has not been fully demonstrated. A key reason for this is that previously investigated materials are non-ideal, and even theoretically do not allow higher efficiency photovoltaics. The GaAsSb/InAs material system is predicted to allow device structures which can experimentally implement a multiple quasi-Fermi level material. The research during this period is focused on the growth of GaAsSb/InAs quantum dots. Highlights of this research included the in-situ observation of the growth of GaAsSb on GaAs via Reflective High Energy Electron Diffraction (RHEED), showing the effect of growth temperature on the growth characteristics. The effect of growth temperature on the morphology of InAs quantum dots was also investigated via AFM studies of uncapped samples. Finally, the role of the strain in grown GaAsSb layers on InAs quantum dot morphology was investigated by varying the Sb content in GaAsSb barrier layers. The overall purpose of this work is the determination of the optimum growth conditions and device designs for the implementation of a quantum dot solar cell using the GaAsSb/InAs materials system.

### **Introduction**

Existing semiconductor devices extensively use band gap engineering to tailor their band structure, and the band edges or energy levels may substantially. However, while a device may (and typically does) contain many energy levels, even at a particular spatial location, a constant among devices is that at a given location and bias point, the absorption and emission properties are dominated by a single quasi-Fermi level. The central requirement of a multiple quasi-Fermi level device is the existence of at least three carrier populations which are not thermalized with each other. For example, in a typical quantum well or quantum dot device, rapid transitions

**20080502068**



between the carrier in the well and in the barrier result in the device and its many energy levels best being described by a single quasi-Fermi levels.

In order to implement a multicolor device, the band structure, density of states and quantum mechanical transition probabilities must be designed such that at least at a single point in the device, there are be multiple quasi-Fermi levels, which allow the simultaneous emission of multiple wavelength peaks, and these peaks should have similar magnitudes. The requirement of similar magnitudes of the emission of the multiple wavelengths peaks is central to realizing the novel properties of a multiple quasi-Fermi level material. There has been some evidence that there is a spatial variation in the quasi-Fermi levels in quantum well devices, as well as evidence for the existence of three absorption transitions, although not three separate quasi-Fermi levels.

One central impediment to the development of multiple quasi-Fermi level materials is the design of a quantum dot device using the appropriate material system. Our previous modeling has shown that material systems which have previously been investigated, primarily the (Al)GaAs/InAs barrier/dot system, are not theoretically ideal and do not result in a higher efficiency solar cell. One major non-ideality in the system is that the (Al)GaAs/InAs system has a large valence band offset. The valence band offset translates directly into a loss in open circuit voltage. Further, the carrier confinement in the valence band increases the transition probabilities between the energy levels in the dot and the valence band, making it more difficult to balance the radiative and emission fluxes between the valence and conduction band via the dot energy levels.

Our previous modeling has shown that several potentially ideal material combinations exist, as shown in Table 1. These material calculations do not include factors such as strain and assume spherical quantum dots, and hence are primarily indicative of which materials systems are promising for further investigation. Further analysis of these materials highlights the GaAsSb barrier/ InAs quantum dot system. This system, depending on the strain, quantum dot size and shape, and composition has a transition from a Type I heterojunction to a Type II heterojunction, thus indicating its suitability for a multiple quasi-Fermi level system. Two avenues must be explored for this material system. First, the growth of the GaAsSb/InAs quantum dot system must be developed, and the focus of this report is on the understanding of the growth mechanisms and growth optimization. A second goal is to develop detailed band structure modeling based on k.p calculations which including strain and the impact of quantum dot shape, both to identify the precise material compositions and also to calculate how material and structural parameters affect the electrical parameters such as density of states and absorption.

**Table 1: Material combinations for demonstrating multiple quasi-Fermi levels.**

Barrier	x	QD	y
GaAs <sub>1-x</sub> Sb <sub>x</sub>	[0, 0.06]	InAs <sub>y</sub> P <sub>1-y</sub>	[0.40, 0.68]
		InP <sub>1-y</sub> Sb <sub>y</sub>	[0.15, 0.25]
Ga <sub>1-x</sub> In <sub>x</sub> As	[0, 0.08]	InAs <sub>y</sub> P <sub>1-y</sub>	[0.40, 0.52]
		InP <sub>1-y</sub> Sb <sub>y</sub>	[0.15, 0.19]
Al <sub>1-x</sub> In <sub>x</sub> As	~ 0.50	InAs <sub>y</sub> P <sub>1-y</sub>	~ 0.40
		InP <sub>1-y</sub> Sb <sub>y</sub>	~ 0.15



## **GaAsSb/InAs material system**

The GaAsSb/InAs system is of interest due to the presence of a zero valence band offset inferred at a Sb content of ~12%. There are a number of other properties of this materials system that make it advantageous for the implementation of a quantum dot solar cell. These include the surfactant effect of the presence of Sb reported in several studies.

There are, however, a number of growth issues that arise when growing GaAsSb layers related to the presence of two Group V elements. Group V elements are volatile with careful control of the flux required via a valve arrangement. They also readily exchange with each other at the growth front. This means that the composition of the GaAsSb depends not just on the Group V fluxes but also the growth temperature. Since the GaAsSb layers will in general not be lattice matched to the growth substrate, strain is also an influence in the growth of GaAsSb layers.

The growth of InAs quantum dots by Stranski-Krastanov mode relies on the strain between barrier and quantum dot material. It therefore stands to reason that the strain present in the GaAsSb barrier layers, determined by the Sb content and layer thickness, will influence the morphology of any quantum dots grown. Finally, the growth temperature will influence the quantum dot properties since it controls the mobility of In on the growth surface and so the ability for congregation of material into larger islands.

The influence of all these factors has been studied and the results will now be outlined in the following sections.

### **RHEED of GaAs<sub>1-x</sub>Sb<sub>x</sub> growth:**

The growth details of strained GaAs<sub>1-x</sub>Sb<sub>x</sub> layers on GaAs substrate were studied by RHEED beam intensity oscillation as a function of substrate temperature and Sb/As flux ratio, to reveal some interesting features which may be important in understanding the growth mechanisms in lattice mismatch system of GaAs<sub>1-x</sub>Sb<sub>x</sub> on GaAs. Figure 1 shows a typical RHEED specular beam intensity oscillation of GaAs<sub>1-x</sub>Sb<sub>x</sub> / GaAs at Sb/As flux ratio of 0.06, as a function of the substrate temperature. The growth of GaAs<sub>1-x</sub>Sb<sub>x</sub> on GaAs shows damped oscillation over the temperature range from 475 °C to 580 °C, which is strongly dependent on the substrate temperature and flux ratio. The RHEED oscillations at different Sb/As flux ratios from 0.06 to 0.02, indicate that both RHEED intensity and RHEED oscillation cycles are reduced with decreasing of substrate temperature and flux ratio. Also asymmetry of the oscillation peak increases as the substrate temperature decreases, which might indicate insignificant incorporation or segregation of Sb at lower temperature. The waveform of RHEED oscillation changes probably reflect the growth kinetics and mechanism, such as growing islands, changes in step and terrace width distributions, which are closely related to lattice mismatch induced strain at the growth front. During layer-by-layer initial growth stage before reaching a critical thickness of GaAs<sub>1-x</sub>Sb<sub>x</sub> on GaAs, a compressive strain by lattice mismatch increases as layer coverage increasing, inhibits cation migration, causes growth front roughen, thus results in decreasing of RHEED intensity. But the mechanism of strain accommodation may change with the substrate temperature and Sb/As flux ratio, this might be the reason causing the different RHEED oscillation behaviors.

The slight variation of growth rate of GaAs<sub>1-x</sub>Sb<sub>x</sub> on GaAs over the temperature range between 580 °C and 450 °C is probably caused by surface desorption and segregation of Sb and As. The

growth rate is slightly increased with decreasing of the substrate temperature at higher Sb/As flux ratio.

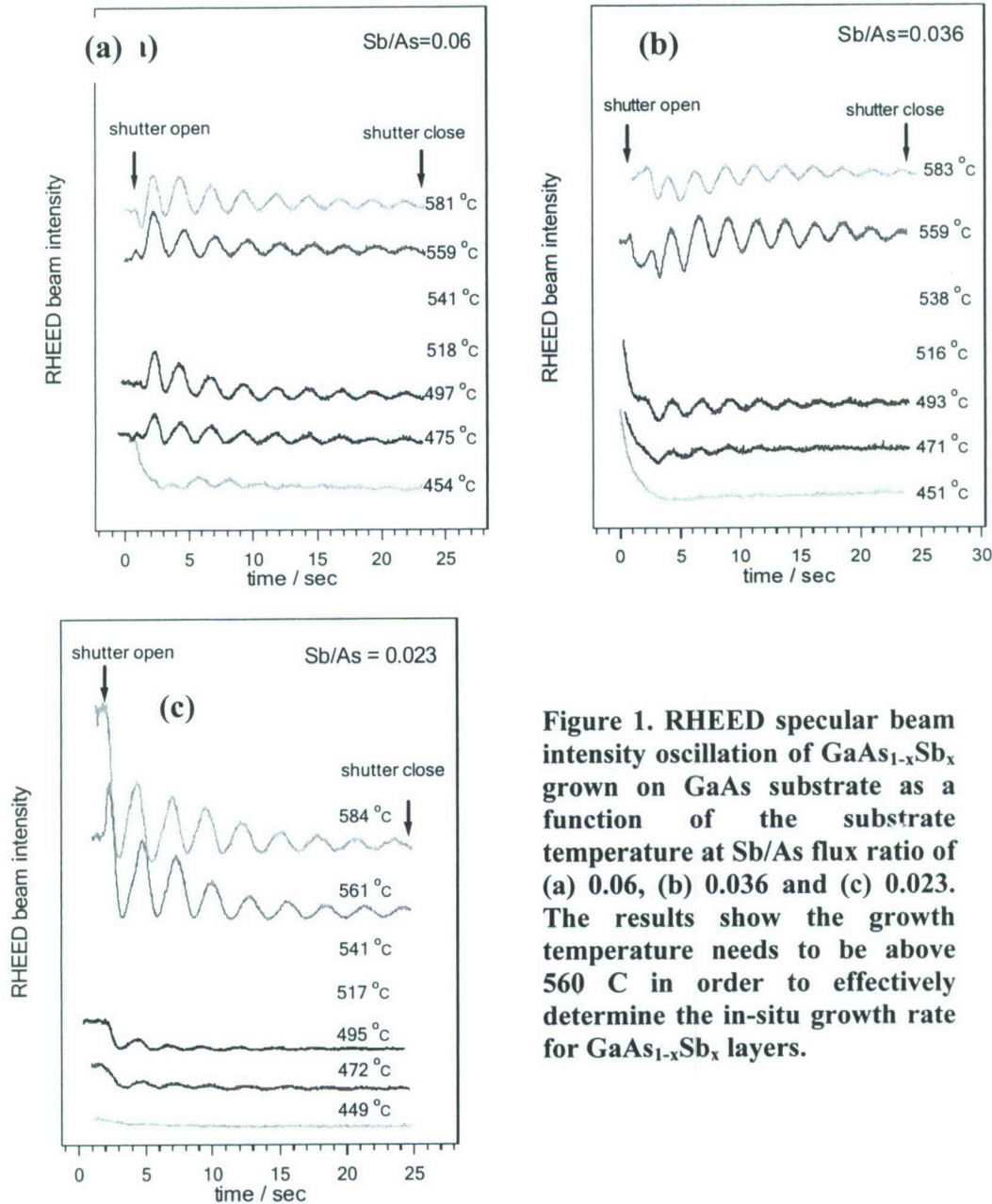


**Figure 1. RHEED specular beam intensity oscillation of  $\text{GaAs}_{1-x}\text{Sb}_x$  grown on GaAs substrate as a function of the substrate temperature at Sb/As flux ratio of (a) 0.06, (b) 0.036 and (c) 0.023. The results show the growth temperature needs to be above 560 C in order to effectively determine the in-situ growth rate for  $\text{GaAs}_{1-x}\text{Sb}_x$  layers.**

#### Effects of surface stain on properties of QDs:

In the case of the GaAs (5 ML) /  $\text{GaAs}_{1-x}\text{Sb}_x$  (5 nm) / GaAs buffer layer in this study, the top 5 ML GaAs layer also included many Sb atoms since the surface exchange reaction occurs between Sb and As atoms and also diffusion of the Sb atoms occurs during MBE growth of the



GaAs on  $\text{GaAs}_{1-x}\text{Sb}_x$  buffer layer. The active surface exchange reaction induces broadening of the GaAs /  $\text{GaAs}_{1-x}\text{Sb}_x$  heterointerface. The Sb atoms diffused from the  $\text{GaAs}_{1-x}\text{Sb}_x$  layer are incorporated into the 5 ML thick GaAs top layer. With increasing of Sb composition in  $\text{GaAs}_{1-x}\text{Sb}_x$  interlayer, the lattice mismatch of InAs layer with the  $\text{GaAs}_{1-x}\text{Sb}_x$  buffer layer is reduced. Accordingly, the strain in the InAs overlayer decreases as the Sb composition increases. This causes the lowering of the hopping barriers, an enhanced diffusion of In adatoms. The lateral ordering of InAs QDs would be determined by the resulting step patterns since the 3D aggregation initiates primarily by the formation of nuclei at the upper edge of steps and large 2D islands of the wetting layer. Thus we would expect that different Sb composition in  $\text{GaAs}_{1-x}\text{Sb}_x$  interlayer leading to different morphologies in arrays of QDs.

Figure 2 shows AFM images of the InAs QDs grown on the GaAs (5 ML) /  $\text{GaAs}_{1-x}\text{Sb}_x$  (5nm) buffer layers with various Sb compositions at 0, 7%, 11%, 19%, and 23%, respectively. The dot density and dot size strongly depend on the Sb surface composition of the GaAs /  $\text{GaAs}_{1-x}\text{Sb}_x$  layer, that is, the density increases, with increasing Sb surface concentration. Meanwhile dot size significantly decreases with increasing of Sb concentration. At this growth condition, the dot density is about  $1.7 \times 10^{10} \text{ cm}^{-2}$  on the conventional GaAs buffer layer. The dot density increased with increasing Sb composition of the  $\text{GaAs}_{1-x}\text{Sb}_x$  buffer layer and reached the value of about  $2.6 \times 10^{10} \text{ cm}^{-2}$  at 23% of Sb composition with low InAs coverage (2 ML). As previously

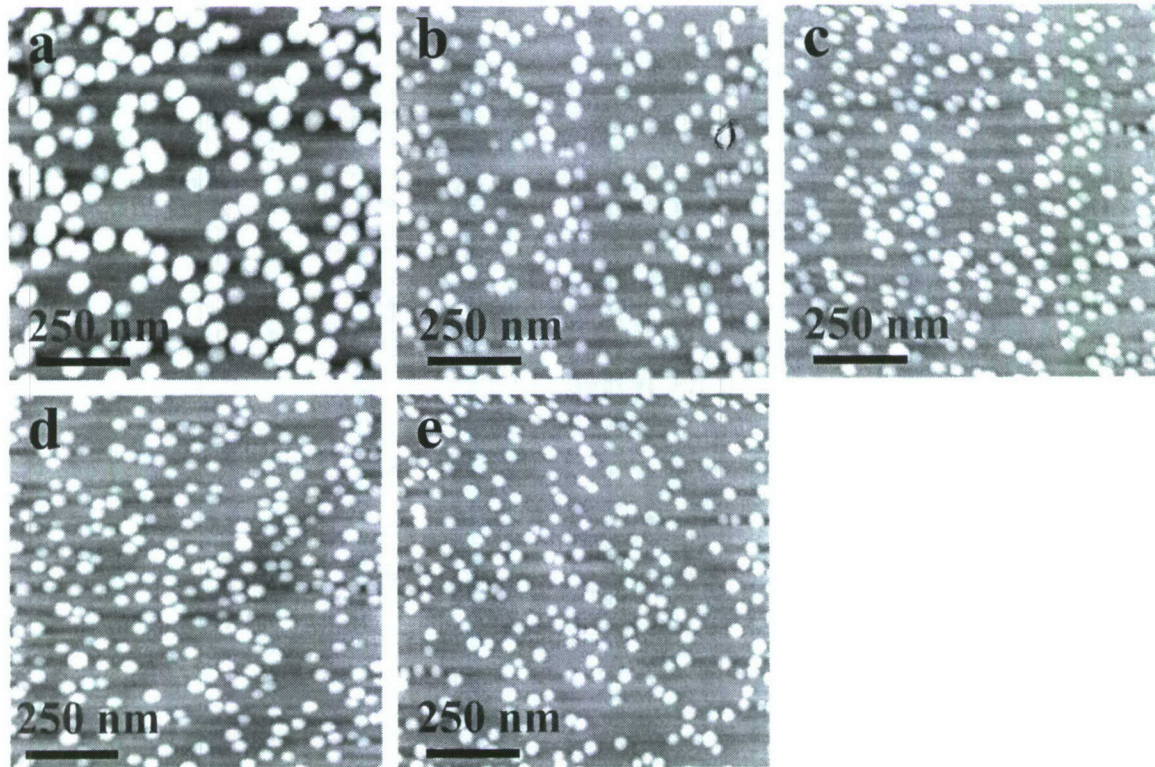


**Figure 2.** AFM images of InAs QDs grown on the GaAs (5 ML) /  $\text{GaAs}_{1-x}\text{Sb}_x$  (5nm) buffer layers with various Sb compositions at 0 (a), 7% (b), 11% (c), 19% (d), and 23% (e), respectively



reported, the Sb surface atoms terminated on the GaAs layer induced a number of 2D wirelike structures and 2D small islands on the surface during the 2D growth of the InAs. These 2D island structures provide numerous step sites, which are preferential sites for 3D nucleation. As a result, the dot density increased on the Sb/GaAs buffer layer. The average lateral size of InAs QDs grown at 23% Sb composition is about 26 nm, which is much smaller in comparison of that of 40 nm grown on conventional GaAs. Surprisingly, the dot size distribution is also improved at higher Sb concentration, which is probably due to the surfactant effect of Sb diffused to the top layer of GaAs. It should be noted that coalescence of neighbouring dots is effectively suppressed in spite of high dot density. As antimony is known to reduce surface energy, these phenomena can be attributed to changes of surface and interface energy.

This last result opens the prospect of controlling dot nucleation through the manipulation of the strain field. Even though this behavior is not yet fully understood, the study of the effects of strain can help improve understanding of ways to control the shapes and sizes of QDs.

### Effects of growth temperature on properties of QDs

In order to study the dot density and dot size dependence on the growth temperature, sample structures with a fixed InAs deposition thickness of 2 ML were grown on a strained GaAs (5 ML) /  $\text{GaAs}_{0.81}\text{Sb}_{0.19}$  buffer layer. Figure 3 shows a series of AFM images of various growth temperatures from 450 °C to 520 °C. From the images, it is clear that the QDs size increases and the density decreases as the growth temperature is raised. Dot density and dot size are both changed dramatically with growth temperature. By increasing the growth temperature from 450 °C to 530 °C, the dot density is decreased up to about 2 orders of magnitude and the dot diameter is increased by a factor of two. At 500 °C, InAs dots with an average area dot density of  $1.8 \times 10^{10} \text{ cm}^{-2}$  and average lateral size of about 28 nm are obtained. At low temperatures below 500 °C, the dots grown have a low aspect ratio below 0.10, it becomes smaller and denser as the temperature decreases. When the temperature reaches 450 °C, the dots formed are extremely dense and some aggregate together to form big islands (about 50-80 nm) among the small dots, as shown in Figure 3a. At high temperature over 500 °C, large dots with heights over 8 nm appear, the large dots have a high aspect ratio above 0.2. No dots could be found in the AFM image when the temperature reaches much higher value above 550 °C. This might be caused by desorption of In adatoms from growth surface, which restrains the dot formation. The appearance of high aspect ratio dots is caused by its volume increasing with rising growth temperature since the energy for a high aspect ratio is lower than that for a low aspect ratio above the critical volume. This means when the area of the dot bottom, at which the compressive strain is introduced from the substrate, becomes large the stress in the dot is relaxed by forming the high aspect ratio shape.

Low area dot density and large dot size indicate high surface diffusion of adatoms at high growth temperatures. This observation is in well agreement with previous predictions that the mechanism behind dot formation via the SK growth method is surface diffusion. At high growth temperatures, the dot formation is kinetically enhanced because adatoms can diffuse longer distances before they accumulate and only large dots with low density occur. The origin of different dot sizes at low temperatures may be attributed to a complex interplay of strain effects, composition, flow rate fluctuation and surface morphology in the SK growth method. The AFM results show that highly uniform dots are only formed under the conditions of high growth



temperatures above 500 °C. The dot size distribution becomes more homogeneous because the surface adatoms have higher mobility at higher temperature than that at lower temperature.

However, when the growth temperature reaches 520 °C, the surface of strained buffer layer starts to form some nanoholes and nanogrooves. The depth of these nanoholes and nanogrooves is more than 3 nm. This indicates that the nanoholes and nanogrooves are formed not only just in the top GaAs (5 ML) layer, but also deep in the strained GaAsSb buffer layer. Therefore, the formation of the nanoholes and nanogrooves is probably caused by desorption of the surface segregated Sb or unstabled GaAsSb at high temperature during the InAs growth. As the InAs growth temperature decreases, the density of the nanoholes and nanogrooves is significantly reduced and they completely disappear when the temperature is below 510 °C. Most of the nanoholes and nanogrooves are located next to the dots, which may indicate the desorbed Sb reforms some small islands or nucleation centers at the edges of nanoholes, providing the preferential sites for the 3D nucleation.

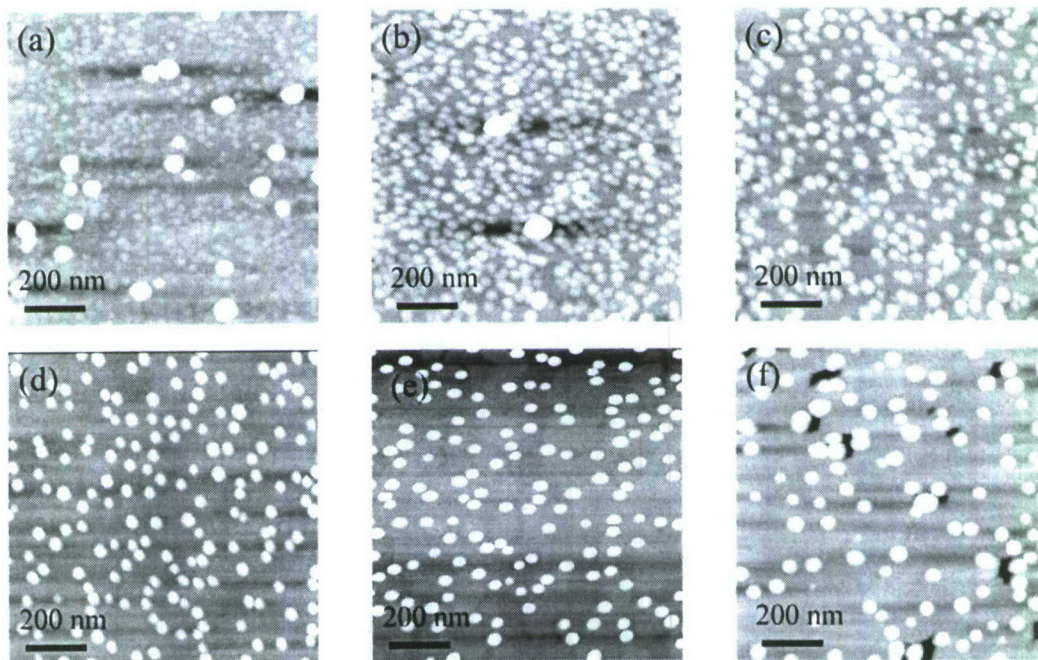


**Figure 3.** AFM images of InAs QDs grown on the GaAs (5 ML) / GaAs<sub>1-x</sub>Sb<sub>x</sub> (5nm) buffer layers at different substrate temperatures. (a) 450 °C, (b) 475 °C, (c) 490 °C, (d) 500 °C, (e) 510 °C, (f) 520 °C respectively.

## Conclusion

The influence of strain on the growth properties of both GaAsSb and InAs quantum dots grown on GaAsSb has been studied. As well as this the influence of growth temperature on the morphology of InAs quantum dots on GaAsSb was also studied. The results suggest that management of the strain in the grown layers is crucial for controlling the properties of the quantum dots in the GaAsSb/InAs materials system. More work must be done, however, to understand the role of strain in order to properly exploit it in the realization of quantum dot solar cells.